CREB is necessary for synaptic maintenance and learning-induced changes of the AMPA receptor GluA1 subunit

ARTICLE *in* HIPPOCAMPUS · JUNE 2013

Impact Factor: 4.16 · DOI: 10.1002/hipo.22108 · Source: PubMed

6 AUTHORS, INCLUDING:

Silvia Middei
Italian National Research Council
30 PUBLICATIONS **723** CITATIONS
SEE PROFILE

Virve Cavallucci
Foundation Santa Lucia
21 PUBLICATIONS **678** CITATIONS
SEE PROFILE

Marcello D'Amelio
Università Campus Bio-Medico di Roma
62 PUBLICATIONS **3,876** CITATIONS
SEE PROFILE

Hélène Marie
Institut de Pharmacologie Moléculaire et Cell…
35 PUBLICATIONS **1,474** CITATIONS
SEE PROFILE

HIPPOCAMPUS 23:488–499 (2013)

CREB is Necessary for Synaptic Maintenance and Learning-Induced Changes of the AMPA Receptor GluA1 Subunit

Silvia Middei,[1*§] Gry Houeland ,[2§] Virve Cavallucci,[3] Martine Ammassari-Teule,[1] Marcello D'Amelio,[3,4] and Hélène Marie[2*]

ABSTRACT: **The transcription factor cAMP response element binding protein (CREB) is a key protein implicated in memory, synaptic plasticity and structural plasticity in mammals. Whether CREB regulates the synaptic incorporation of hippocampal glutamatergic receptors under basal and learning-induced conditions remains, however, mostly unknown. Using double-transgenic mice conditionally expressing a dominant negative form of CREB (CREBS133A, mCREB), we analyzed how chronic loss of CREB function in adult hippocampal glutamatergic neurons impacts the levels of the AMPA and NMDA receptors subunits within the post-synaptic densities (PSD). In basal (naïve) conditions, we report that inhibition of CREB function was associated with a specific reduction of the AMPAR subunit GluA1 and a proportional increase in its Ser845 phosphorylated form within the PSD. These molecular alterations correlated with a reduction in AMPA receptors mEPSC frequency, with a decrease in long-term potentiation (LTP), and with an increase in long-term depression (LTD). The basal levels other major synaptic proteins (GluA2/3, GluN1, GluN2A, and PSD95) within the PSD were not affected by CREB inhibition. Blocking CREB function also impaired contextual fear conditioning (CFC) and selectively blocked the CFC-driven enhancement of GluA1 and its Ser845 phosphorylated form within the PSD, molecular changes normally observed in wild-type mice. CFC-driven enhancement of other synaptic proteins (GluA2/3, GluN1, GluN2A, and PSD95) within the PSD was not significantly perturbed by the loss of CREB function. These findings provide the first evidence that, in vivo, CREB is necessary for the specific maintenance of the GluA1 subunit within the PSD of hippocampal neurons in basal conditions and for its trafficking within the PSD during the occurrence of learning.** © **2013 Wiley Periodicals, Inc.**

KEY WORDS: **glutamatergic receptors; memory formation; synaptic plasticity; transcription factor; hippocampus**

[1] **Institute of Cellular Biology and Neurobiology, National Research Council, IRCCS, Santa Lucia Foundation, Rome, Italy;** [2] **Laboratory of Molecular Mechanisms of Synaptic Plasticity, European Brain Research Institute, Rome, Italy;** [3] **IRCCS, Santa Lucia Foundation, Rome, Italy;** [4] **Laboratory of Molecular Neuroscience, University Campus Biomedico, Rome, Italy**

[§]Silvia Middei and Gry Houeland contributed equally to this work.

Additional Supporting Information may be found in the online version of this article.

Grant sponsors: Regione Lazio Sviluppo della Ricerca sul Cervello, Italian Institute of Technology, American Alzheimer Association, PRIN 2009 (Projects for Research of National Interest); Grant sponsor: Alzheimer's Association; Grant number: NIRG-11-204588.

*Correspondence to: Silvia Middei, Institute of Cellular Biology and Neurobiology, Via del Fosso di Fiorano 64, 00143 Rome, Italy. E-mail: s.middei@hsantalucia.it or Hélène Marie, IPMC—CNRS UMR7275, 660 Route des Lucioles, Sophia-Antipolis, 06560 Valbonne, France. E-mail: marie@ipmc.cnrs.fr

Accepted for publication 31 January 2013
DOI 10.1002/hipo.22108
Published online 18 March 2013 in Wiley Online Library (wileyonlinelibrary.com).

INTRODUCTION

There is now accumulating evidence that the increased number and availability of glutamatergic receptors, via their translocation to hippocampal synaptic sites, control the stabilization of memory traces (Rumpel et al., 2005; Matsuo et al., 2008). Dendritic spines, the postsynaptic sites of excitatory synapses, are the main loci for this molecular reorganization as they contain the post-synaptic density (PSD), a dense structure including adhesion molecules and slots for the insertion of receptors. In vivo evidence reports that training in hippocampus-dependent memory tasks leads to the incorporation of glutamatergic AMPA receptors (AMPARs) in the PSD compartment of dendritic spines (Rumpel et al., 2005; Matsuo et al., 2008). Similar molecular changes believed to support learning have been characterized in vitro such as long-term potentiation (LTP) and long-term depression (LTD) of AMPAR transmission (Malenka and Bear, 2004). In particular, in the hippocampus, LTP is at least partially due to phosphorylation of the GluA1 subunit of AMPARs leading to its delivery to synapses, whereas LTD requires dephosphorylation of GluA1 leading to endocytosis of AMPARs (Lu and Roche, 2012).

The transcription factor cAMP response element binding protein (CREB) is involved in memory formation and synaptic plasticity (Barco and Marie, 2011). Enhancing CREB-dependent transcription in the hippocampus in vivo increases hippocampus-dependent memory formation (Restivo et al., 2009; Sekeres et al., 2010), increases LTP (Barco et al., 2002; Marie et al., 2005; Marchetti et al., 2011) and increases spinogenesis (Marie et al., 2005). Inhibiting CREB function perturbs hippocampus-dependent memory formation (Barco et al., 2002; Kida et al., 2002; Pittenger et al., 2002; Mamiya et al., 2009) and inhibits LTP (Pittenger et al., 2002; Huang et al., 2004; Jancic et al., 2009). Although these findings strongly suggest that CREB could be implicated in synaptic receptor trafficking, the necessity of this transcription factor in this process under basal conditions and during hippocampus-dependent learning has not yet been addressed.

Using mice conditionally expressing a dominant negative form of CREB (CREBS133A) in forebrain neurons (named hereafter mCREB mice) (Newton et al., 2002), we previously reported that blocking CREB function impairs hippocampus-dependent contextual fear conditioning (CFC) and perturbs the dendritic spine rearrangements of hippocampal circuits normally occurring during this memory task (Middei et al., 2012). These recent data support the idea that CREB might also be involved in the incorporation of postsynaptic receptors that accompany spine rearrangements during learning. To further investigate this point, we now used these same mCREB mice to examine the impact of CREB inhibition on AMPAR and NMDA receptor (NMDAR) trafficking under both basal (naïve) and learning-dependent (CFC) conditions.

We report that, under naïve conditions, loss of CREB function specifically perturbed the maintenance of synaptic AMPARs within the PSD, lowered AMPAR miniature excitatory post-synaptic current (mEPSC) frequency, and favored LTD. CREB inhibition also disrupted CFC and selectively blocked the CFC-evoked enhancement of GluA1 PSD levels and PSD levels of its serine 845 phosphorylated form, molecular alterations normally observed in wild-type (WT) mice. These findings provide the first evidence that CREB is necessary for the basal and learning-induced regulation of AMPAR trafficking in vivo.

MATERIALS AND METHODS

Transgenic Mice

Forebrain expression of mCREB dominant negative mutation (serine 133 to alanine mutation, S133A) was achieved by crossing mice bearing the mCREB mutation under the control of the tetracycline-operated promoter [tetOp-mCREB mouse line, (Newton et al., 2002)] with mice expressing the tetracycline transactivator (tTA) under the control of the α-calmodulin Kinase II (αCaMKII) promoter [αCaMKII-tTA mouse line, (Mayford et al., 1996)]. Both lines were on C57BL/6J mice transgenic background. Litters were genotyped for expression of the two transgenes by PCR. To avoid abnormal development of the double transgenic mice, mCREB expression was prevented by treatment of all litters with food containing 40 mg/Kg doxycycline (Bio-Serv) during the last week of pregnancy and from birth to weaning (post-natal day 21). Upon weaning, mCREB expression was induced by removing doxycycline from the diet. All experiments were performed on 8–15 weeks old mice, allowing for several weeks of transgene expression in mCREB mice. Control data were obtained in WT littermates. When necessary, mice were transcardially perfused under deep anesthesia (ketamine/xylazine, 100 and 15 mg/kg, respectively). Reversal experiments were performed on adult (10–11 weeks) mCREB and WT mice 10 days after doxycycline diet administration (40 mg/Kg). Mice were housed in accordance with the guidelines laid down by the European Communities Council Directive (86/609/EEC). All experiments were carried out under a licence issued by the Local Animal Ethics Committee and performed by an experimenter blind to the animals' genotype and condition.

Immunohistochemistry for pCREB

WT and mCREB mice were transcardially perfused with 4% paraformaldehyde 60 min after the CFC test phase or directly after being collected from their home cage (naïve). Brains were quickly removed, post-fixed in paraformaldehyde overnight, cryoprotected, frozen and sectioned into 40 μm slices. Floating slices were incubated with an antibody against Ser-133 phosphorylated CREB (rabbit anti-Phospho-CREB, Upstate, NY) at a 1:200 concentration and stained according to the Ultra tek HRP kit instructions (Scy Tek laboratories). The peroxidase reaction end product was visualized with diaminobenzidine (50 mg/100 ml of PBS) in the presence of 0.02% hydrogen peroxide for 6 min. After processing, immunolabeled sections were washed in phosphate buffer, mounted onto gelatin-coated slides, and dehydrated through alcohol to toluene for light microscopical examination. Digital images were acquired at 4× magnification for whole hippocampus visualization and 20× magnification for focus on CA1 hippocampal region. The quantification of pCREB-positive cells within the CA1 pyramidal cell body layer was carried out by measuring optical density on digitalized images. Optical densities of areas including labelled cells above a threshold determined from control region were counted with ImageJ software. Seven to thirteen serial sections were digitized and analyzed for each animal.

Western Blotting

Mice were sacrificed 24 h after the end of test phase for the CFC and pseudo-trained conditions. Naïve mice were taken directly from their home cage for scarification and processed identically.

For total hippocampal homogenate preparations, hippocampi were collected and homogenized in lysis buffer (320 mM sucrose, 50 mM NaCl, 50 mM Tris-HCl pH 7.5, 1% Triton X-100, 0.5 mM Na_3VO_4, 5 mM β-glycerophosphate, 1 mM EDTA, 1 mM $NaHCO_3$, 1 mM PMSF, 1 mM Na_3VO_4, 5mM NaF, protease inhibitor cocktail), incubated on ice for 30 min and centrifuged at 13,000*g* for 10 min. The total protein content of the resulting supernatant was determined by the Bradford method. Quantitative analysis of all proteins in total homogenates was performed using β-tubulin (1:10,000, Sigma) as a loading control.

For PSD isolation, hippocampi were homogenized in a homogenization buffer (320 mM sucrose, 10 mM Tris-HCl pH 7.4, 1 mM EDTA, 1 mM $NaHCO_3$, 1 mM PMSF, 1 mM Na_3VO_4, 5 mM NaF, protease inhibitor cocktail) with 10 strokes of a tight-fitting glass Dounce tissue grinder. The homogenate was centrifuged at 1,000*g* for 10 min and the resulting supernatant was centrifuged at 10,000*g* for 15 min. The pellet was resuspended in the homogenization buffer containing 0.5% Triton ×100, incubated 40 min on ice, and centrifuged at 32,000*g* for 20 min. The resulting pellet

enriched in PSDs was resuspended in RIPA buffer (50 mM Tris-HCl pH 7.4, 1% Triton X-100, 0.25% Na-deoxycholate, 150 mM NaCl, 5 mM $MgCl_2$, 1 mM EDTA, 0,1% SDS, 1 mM Na_3VO_4, 5 mM β-glycerophosphate, protease inhibitor cocktail), sonicated and incubated on ice for 20 min. The samples were centrifuged at 11,500*g* for 10 min and the protein concentration of the resulting supernatant was determined. Successful enrichment of PSDs was confirmed by presence of PSD95 and absence of synaptophysin in extracts as described previously (data not shown) (D'Amelio et al., 2011). Equal amounts of proteins were applied to SDS-PAGE and electroblotted on a PVDF membrane. PSD fractions from all samples analyzed were also separated by SDS-PAGE and stained with Coomassie brilliant blue. No differences in pattern distribution and amount of PSD proteins were detected (Supporting Information Fig. S1). Immunoblotting analysis was performed using a chemiluminescence detection kit (Millipore). Primary antibodies: GluA1 (clone C3T, 1:1,000, Upstate/Millipore 04-855), pGluA1Ser845 (1:1,000, Chemicon/Millipore AB5849), pGluA1Ser831 (1:1,000, Upstate/Millipore 04-823), GluA2/3 (1:1,000, Chemicon/Millipore AB1506), GluN1 (NMDAζ1; 1:500, Santa Cruz sc-1467), GluN2A (NMDAϵ1; 1:500, Santa Cruz sc-1468), PSD-95 (1:2,000, Chemicon/Millipore MAB1598). The relative levels of immunoreactivity were determined by densitometry using the software ImageQuant 5.0.

Electrophysiology

Experimental days recording from mCREB and WT mice were generally interleaved. 400 μm transverse hippocampal slices were prepared for electrophysiology using standard procedures (Marchetti et al., 2010) and incubated in ACSF containing (in mM): 119 NaCl, 26 $NaHCO_3$, 2.5 KCl, 1.00 NaH_2PO_4, 1.3 $MgSO_4$, 2.5 $CaCl_2$, 11 glucose, gassed with 95%O_2/5%CO_2, pH7.4, and recorded at 32 ± 1°C in presence of 100 μM picrotoxin (Sigma-Aldrich, Italy) to block inhibitory GABAergic transmission.

fEPSPs were generated by stimulating the Schaffer collateral pathway to CA1 pyramidal neuron synapses (SC-CA1 synapse). Stimulating electrodes (monopolar glass pipettes filled with ACSF) and recording electrodes (filled with 1 mM NaCl + 10 mM HEPES, pH = 7.4) were placed in the CA1 stratum radiatum. Input/output (I/O) curves were generated in response to stimulation intensities of 10–50 μA/0.1 ms (in 10 μA increments, 10 sweeps average). For paired pulse ratios (PPR), a fEPSP of about 50% of the maximum amplitude was obtained and two stimuli were delivered at 50, 100, 200, 300, and 400 ms inter-stimulus intervals (ISI). PPRs were calculated as slopeEPSP2/slopeEPSP1 (10 sweeps average per ISI). LTP was induced using a standard high frequency stimulation protocol (100 Hz for 1 s) after 15 min of stable fEPSP slope (0.1 Hz stimulation) set at approximately 30% of maximum amplitude. LTD experiments were performed in ACSF containing 4 mM $CaCl_2$/2mM $MgSO_4$ to favor LTD induction and induced by a standard low frequency stimulation protocol (900 pulses at 1 Hz) after 15 min of stable fEPSP slope (0.05 Hz stimulation) set at ~50% of maximum amplitude. fEPSP slope values were averaged in one minute bins and then averaged per slice over time periods analyzed.

To measure mEPSCs, CA1 pyramidal cells were voltage clamped at −65 mV holding potential. For these recordings, the ACSF was slightly modified to $[Ca^{2+}]$ = 4 mM and $[K^+]$ = 7 mM, in the presence of 0.5 μM tetrodoxin (TTX, Latoxan, France) and 50 μM APV (Tocris, UK). Whole-cell patch clamp recordings were carried out using the following intracellular solution: 117.5 mM $CsMeSO_4$, 15.5 mM, CsCl, 10 mM TEACl, 8 mM NaCl, 1.25 mM NaH_2PO_4, 10 mM HEPES, 0.25 mM EGTA, 4 mM MgATP, 0.3 mM NaGTP, pH= 7 .3, osmolarity ~290 mOsm.

Recordings were made using a Multiclamp 700B amplifier (Axon Instruments) and digitized through a National Instruments BNC-2090 board with Igor Pro Software (Wavemetrics). Data were analyzed using Clampfit (PCLAMP, Axon Instruments). mEPSCs were analyzed using a template search with variable amplitude.

CFC

Mice were handled in the experimental room for 3 days. On the 4th day, they were trained in the conditioning chamber (square cage: dimensions 28 × 28 cm^2 with transparent walls). Training consisted in 2 min habituation before the delivery of five foot shocks (0.7 mA, 2 s) at 1 min intervals. One minute after the last foot shock mice returned to their home cage. Context conditioning was assessed 24 h after the training by placing mice for 5 min in the conditioning chamber. A group of WT mice underwent pseudo-training, consisting in putting mice for 7 min in the conditioning chamber without the delivery of foot shocks. Mouse behavior was videotaped and fear memory was manually assessed by scoring the total amount of freezing behavior (defined as complete lack of movement, except for respiration) over the 5 min test. Values are reported as % of time spent freezing.

Statistical Analysis

All studies were performed by experimenters blind to the genotypes and experimental conditions of animals. Immunohistochemical measurements on naïve mice and CFC trained mice were compared among groups by means of a two-way ANOVA with genotype and condition as between factors and confirmed by one-way ANOVAs where necessary. All AMPARs and NMDARs subunits and PSD-95 from mice on naïve conditions were compared among groups by means of one-way ANOVAs with genotype as between factor. Electrophysiological data were statistically analyzed using an unpaired two-tailed Student's *t*-test (Prism, GraphPad). CFC performance during training and test and compared among genotypes by means of one way ANOVAs. All AMPAR and NMDAR subunits and PSD-95 from mice after training in CFC were compared among groups including the data collected on naïve animals by means of two-way ANOVAs with genotype and condition as between factors. Bonferroni post hoc tests were then used for

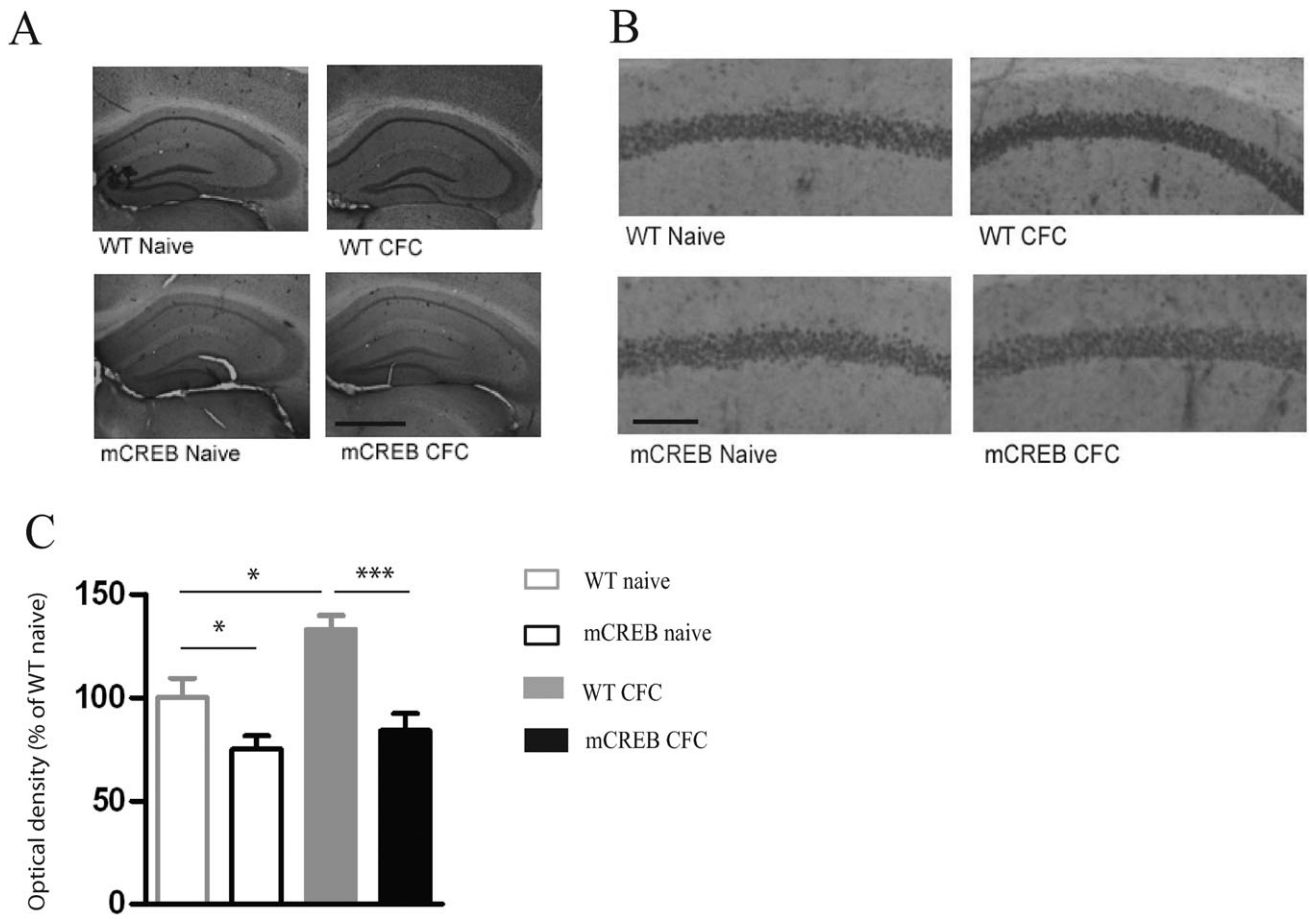

FIGURE 1. mCREB expression reduces basal and learning-induced CREB phosphorylation (A-B) Images of phosphorylated CREB (pCREB) staining in mCREB (bottom panels) and WT (top panels) mice under naïve (left panels) and CFC (right panels) conditions for whole hippocampus (A) and CA1 region only (B). Scale bars: 10 µm in A and 1 µm in B. (C) Quantitative analysis of immunocytochemical labelling of pCREB. Basal levels of pCREB were reduced in mCREB mice compared to WT in naïve conditions. CFC induced an activation of pCREB in the CA1 of the dorsal hippocampus in WT mice but not in mCREB mice, when measured 1 h after the CFC test ($N = 3$ mice, $n = 7$–13 slices for each experimental group). Statistics: $^{*}P < 0.05$; $^{***}P < 0.001$.

multiple comparisons where necessary. All differences were considered significant for $P < 0.05$.

RESULTS

Reduced CREB Phosphorylation in the Hippocampus of mCREB Mice

Among the mutations affecting CREB, the mCREB S133A mutation, which prevents CREB phosphorylation, is known to reduce CREB-mediated gene transcription by occlusion of CRE-sites (Carlezon et al., 2005). We previously reported that, in the mCREB transgenic mice used in this study, the mCREB transgene is expressed in forebrain regions including the hippocampus, a region known to have a pivotal role in the formation of contextual memories (Middei et al., 2012). Here, to confirm biological activity of the mCREB transgene, we characterized how learning a CFC task affects the hippocampal levels of phosphorylated CREB in mCREB and WT mice. Adult mCREB double transgenic mice and WT littermates were either collected from the home-cage (naïve mice) and sacrificed immediately or trained in CFC and sacrificed 60 min after the test phase (CFC mice). Immunohistochemical detection of phosphorylated CREB was evaluated in the cell body layer of CA1 pyramidal neurons (Fig. 1A,B) on naïve mice and on mice sacrificed 1 h after the test phase. A two-way ANOVA analysis performed on data showed a significant difference among genotypes (Fig. 1C, $F_{1,142} = 15.32$, $P < 0.001$). One-way ANOVAs confirmed that in naïve conditions, presence of the mCREB transgene reduced the basal levels of pCREB (naïve WT vs. naïve CREB, $F_{1,70} = 5.41$, $P < 0.05$). On samples collected 60 min after the end of the test phase, CFC led to an increase in pCREB levels in WT mice (WT naïve vs. WT CFC, $F_{1,75} = 6.50$, $P < 0.05$), but not in mCREB mice (mCREB naïve vs. mCREB CFC, $F_{1,53} = 0.55$, $P > 0.05$). mCREB mice still exhibited a significant reduction in pCREB after CFC compared to WT (WT CFC vs. mCREB CFC, $F_{1,55} = 14.28$, $P < 0.001$). These data confirm that mCREB expression significantly reduces CREB phosphorylation, and thus CREB function, and that training in a hippocampus-de-

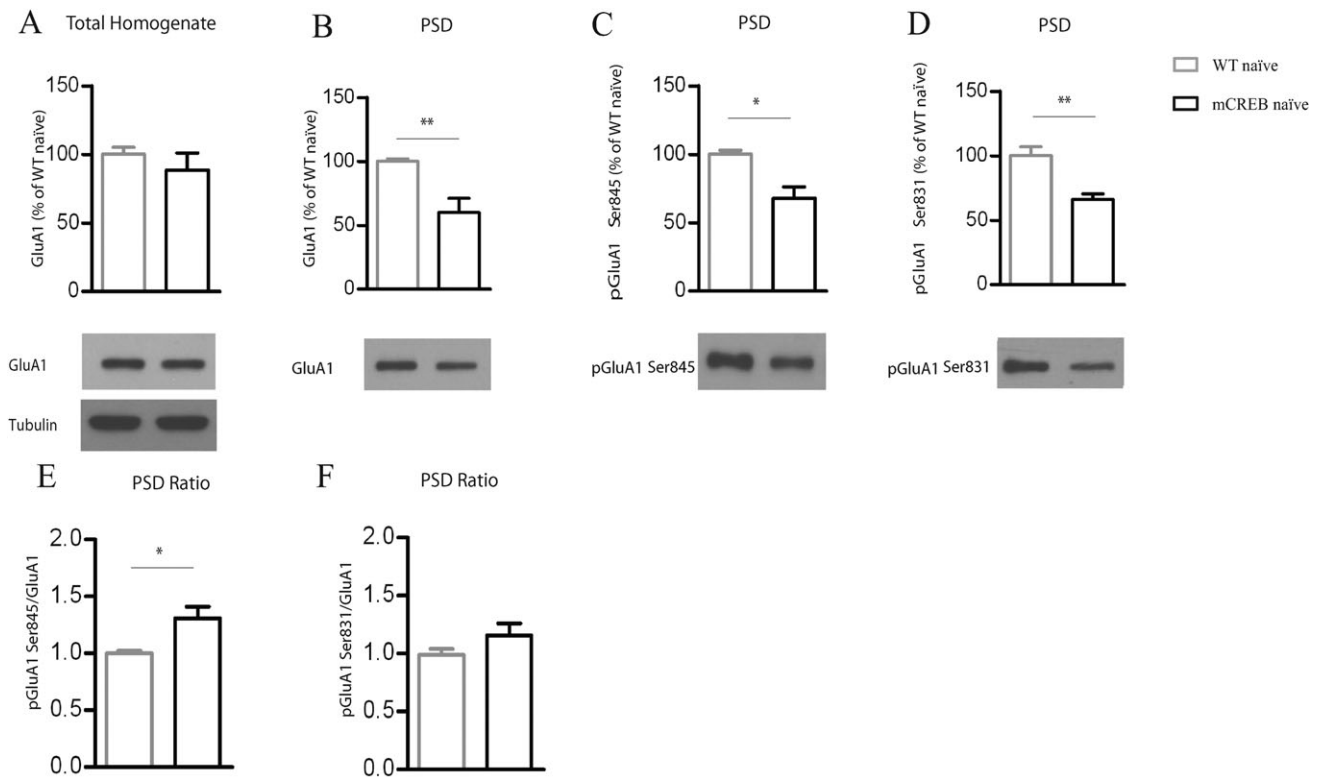

FIGURE 2. In naïve conditions, GluA1 maintenance at the PSD depends on CREB. Quantitative analysis of GluA1 and its phosphorylated forms (S845 and S831) in the hippocampus of naïve mCREB and WT mice. (A–D) Densitometric quantification of changes in gray values expressed as mean (% of average WT naïve) ± s.d. (average WT is indicated as 100%) and representative immunoblots used for quantification. (A) GluA1 levels in total hippocampal extracts (tubulin was used for normalization for total homogenates) (B) GluA1 levels in the PSD; (C) Levels of S845 phosphorylated GluA1 in the PSD; (D) Levels of S831 phosphorylated GluA1 in the PSD; ($n = 3$ mice in each group for total homogenates, $n = 5$ mice in each group for PSDs). (E) Ratio of S845 phosphorylated GluA1 in PSD (data from C) to GluA1 in the PSD (data from B). (F) Ratio of S831 phosphorylated GluA1 in PSD (data from D) to GluA1 in the PSD (data from B). Statistics: $^*P < 0.05$, $^{**}P < 0.01$.

pendent task is associated with increased CREB phosphorylation in WT mice but not in mCREB mice.

In naïve conditions, GluA1 maintenance at the PSD depends on CREB

Despite chronic inhibition of CREB, we previously reported that dendritic spines density and morphology are unaltered in the CA1 hippocampal neurons of mCREB mice (Middei et al., 2012). We now evaluated if this structural stability was reflected by receptor integrity at glutamatergic synapses. We analyzed the levels of the main hippocampal AMPAR subunit GluA1 in total hippocampal homogenates and within the PSD in naïve WT and mCREB mice. We also analyzed the levels of the phosphorylated forms of GluA1 (serine 845 and serine 831) within the PSD as these forms are known to be involved in regulating the biophysical properties of the AMPA receptor and its trafficking during synaptic plasticity (Lu and Roche, 2012). We observed that GluA1 levels in total hippocampal extracts were unaffected by mCREB expression (Fig. 2A; $F_{1,4} = 0.72$, $P > 0.05$), suggesting that CREB does not regulate basal transcription levels of this subunit. There was, however, a significant reduction in PSD GluA1 levels (Fig. 2B; $F_{1,8} = 12.75$, $P < 0.01$), and in PSD levels of GluA1 phosphorylated at Ser845 and Ser831 (Figs. 2C,D; $F_{1,8} = 8.29$, $P < 0.05$ and $F_{1,8} = 17.59$, $P < 0.01$) in mCREB mice compared to WT mice. The ratio of the GluA1-Ser845 phosphorylated form versus total GluA1 within the PSD was enhanced in mCREB mice (Fig. 2E, $F_{1,8} = 8.49$, $P < 0.05$), while the ratio of the GluA1-Ser831 phosphorylated form versus total GluA1 within the PSD was not significantly affected (Fig. 2F, $F_{1,8} = 2.10$, $P > 0.05$). These data suggest that inhibiting CREB specifically disrupts the maintenance of the GluA1 subunit within the PSD and enhances the proportion of GluA1-Ser845 within the PSD.

We also assessed total hippocampal levels and PSD levels of other synaptic proteins (Fig. 3). Blocking CREB function slightly reduced GluA2/3 levels in total extracts (Fig. 3A; $F_{1,4} = 13.9$, $P < 0.05$), but did not perturb the levels of this subunit within the PSD (Fig. 3B; $F_{1,10} = 1.57$, $P > 0.05$). Blocking CREB function did not affect the levels of the two major NMDAR subunits, GluN1 and GluN2A, in total extracts or within the PSD (GluN1: Figs. 3C,D, $F_{1,4} = 0.02$, $P > 0.05$ and $F_{1,8} = 0.19$, $P > 0.05$; GluN2A: Figs. 3E,F, $F_{1,4} = 0.02$, $P > 0.05$ and $F_{1,6} = 0.03$, $P > 0.05$). Expression of the scaf-

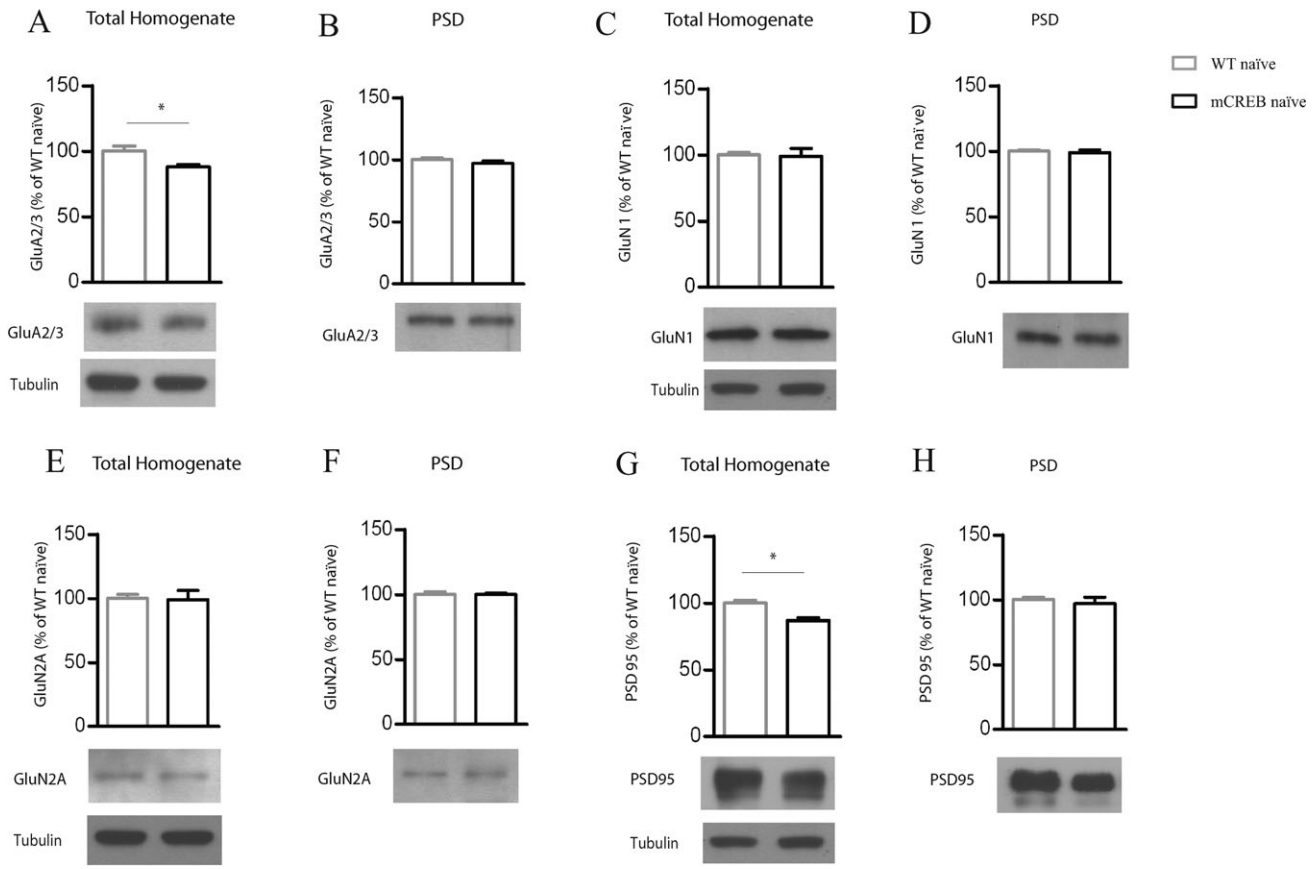

FIGURE 3. In naïve conditions, maintenance of other synaptic proteins at the PSD does not depend on CREB. Quantitative analysis of GluA2/3, GluN1, GluN2A, and PSD95 in the hippocampus of naïve mCREB and WT mice. (A–H) Densitometric quantification of changes in gray values expressed as mean (% of average WT naïve) ± s.d. (average WT is indicated as 100%) and representative immunoblots used for quantification. (A) GluA2/3 levels in total hippocampal extracts (tubulin was used for normalization for total homogenates); (B) GluA2/3 levels in the PSD; (C) GluN1 levels in total hippocampal extracts; (D) GluN1 levels in the PSD; (E) GluN2A levels in total hippocampal extracts; (F) GluN2A levels in the PSD; (G) PSD95 levels in total hippocampal extracts; (H) PSD95 levels in the PSD; ($n = 3$ mice in each group for total homogenates, $n = 4/6$ mice in each group for PSDs). *$P < 0.05$.

folding protein, PSD95, was slightly reduced due to CREB inhibition in total extract (Fig. 3G; $F_{1,4} = 16.86$, $P < 0.05$), but the levels of this protein within the PSD were not affected (Fig. 3H, $F_{1,6} = 1.46$, $P > 0.05$). Overall, these data argue for a possible role of CREB in regulating hippocampal expression of GluA2/3 subunits and PSD95. More importantly, we demonstrate that, in basal conditions, the regulation of PSD levels of GluA1 by CREB is highly specific to this subunit.

mCREB expression lowers AMPAR mEPSC frequency and shifts hippocampal synaptic plasticity toward LTD

We next investigated if this reduction of GluA1 within the PSD could alter glutamatergic transmission and plasticity of the hippocampus in naïve mice using electrophysiology. We first investigated basic synaptic transmission at the schaffer collateral to CA1 pyramidal neuron (SC-CA1) synapse by evaluating the relationship between stimulation strength and field excitatory post-synaptic potentials (fEPSP I/O curves). Synapses from transgenic mice displayed normal transmission using this analysis (Fig. 4A). However, using the more sensitive technique of whole-cell patch clamping, we confirmed that loss of the GluA1 subunit from synapses correlates with an alteration in AMPAR transmission by recording mEPSCs in CA1 pyramidal neurons, which represent AMPAR-mediated post-synaptic responses to spontaneous release of individual glutamate vesicles. Indeed, while AMPAR mEPSC amplitude was not altered (Fig. 4B, left), there was a significant decrease in mEPSC frequency in mCREB mice (Fig. 4B, right; $P < 0.01$). We did not observe any alterations in pre-synaptic release properties as measured by the paired pulse ratio (PPR, Fig. 4C). Together, these data suggest that loss of CREB function induces a specific decrease in the number of AMPAR-containing synapses (AMPAR mEPSC frequency decreased, but no change in PPR), correlating with less AMPAR content in total PSD fractions, but leaving the AMPAR content within the remaining synapses intact (AMPAR mEPSC amplitude unchanged).

Based on previous evidence that the dynamics of GluA1 phosphorylation of S845 are implicated in LTD (Lu and Roche, 2012), we hypothesized that inhibiting CREB might alter LTD in CA1 pyramidal neurons. We investigated synaptic plasticity at the SC-CA1 synapse in naïve WT and mCREB mice. We observed that LTP expression was significantly

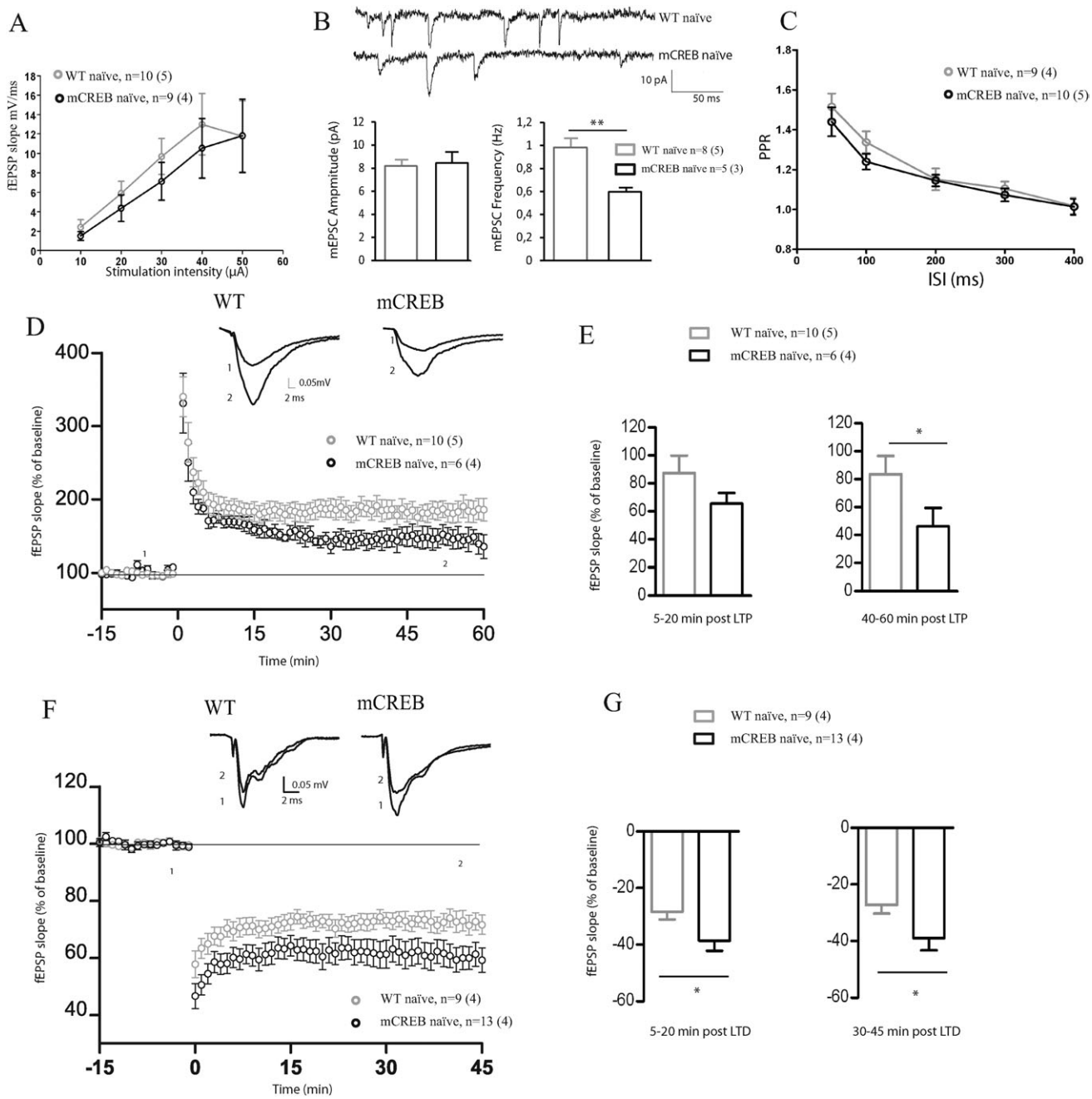

FIGURE 4. Blocking CREB function reduces AMPAR mEPSC frequency, shifts synaptic plasticity toward weaker LTP and stronger LTD. (A) Basic synaptic transmission investigated by fEPSP I/O curves at the Schaffer collateral to CA1 (SC-CA1) synapse of mCREB and WT mice. (B) (Top) Representative traces for naïve WT and mCREB mice are shown displaying spontaneous AMPAR-mediated mEPSCs. (Bottom) Mean ± s.e.m for amplitude and frequency of AMPAR mEPSCs in naïve WT and mCREB mice. (C) Paired pulse ratios (PPR; fEPSP2 slope/fEPSP1 slope) of the SC-CA1 synapse of WT and mCREB mice for 50–400 ms ISI. (D) Summary graphs of LTP (induced at time 0) as % of fEPSP baseline elicited at the SC-CA1 synapse in mCREB and WT mice. Traces above graph show sample fEPSP traces pre-LTP induction (1) and post-LTP induction (2; 40–60 min post). (E) Summary of fEPSP magnitude (% increase of baseline) at 5–20 min and 40–60 min post-LTP induction in WT and mCREB mice. (F) Summary graphs of LTD (induced at time 0) as % of fEPSP baseline elicited at the SC-CA1 synapse in mCREB and WT mice. Traces above graph show sample fEPSP traces pre-LTD induction (1) and post-LTD induction (2; 30–45 min post). (G) Summary of fEPSP magnitude (% reduction of baseline) at –20 min and 30–45 min post-LTD induction in WT and mCREB mice. For B: *n* = cells (mice); for A, D, and F: *n* = slices (mice). **P* < 0.05; ***P* < 0.01.

reduced (Figs. 4D–E; $P < 0.05$), as reported previously in other mice where CREB function was blocked (Barco and Marie, 2011). We, however also observed that LTD was enhanced in mCREB compared to WT mice (Figs. 4F–G; $P < 0.05$). We conclude that inhibiting CREB favors synaptic plasticity mechanisms that are necessary to express LTD.

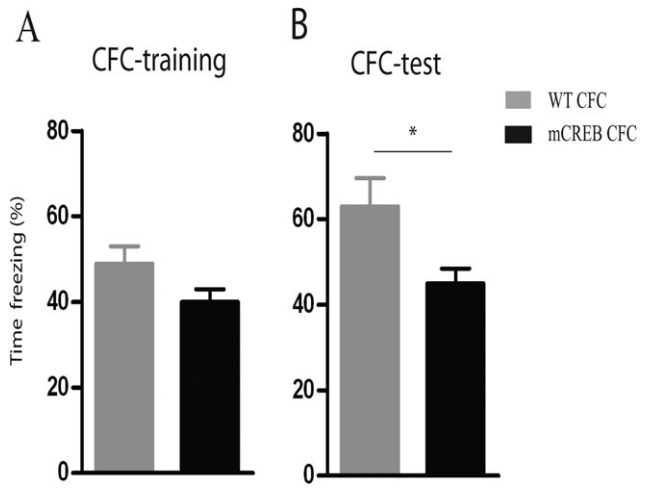

FIGURE 5. CFC is impaired in mCREB mice. Percentage of freezing time during (A) the CFC training and (B) the CFC test displayed by WT and mCREB mice. Data are expressed as mean ± s.e.m; $n = 9$ WT, 6 mCREB. $^*P < 0.05$.

CREB is necessary for learning-induced alterations of GluA1 within the PSD

Having established that chronically blocking CREB function affects glutamatergic synaptic function in naïve conditions, we next examined its impact on PSD modifications after learning. Mice were subjected to hippocampus-dependent CFC and their fear memory was estimated by analyzing the amount of freezing during the test performed 24 h after training. WT and mCREB mice reported the same amount of freezing during training (Fig. 5A, $F_{1,13} = 2.30$, $P > 0.05$). During the test, however, freezing was significantly reduced in mCREB mice compared to WT mice (Fig. 5B, $F_{1,13} = 12.19$, $P < 0.05$), confirming that blocking CREB function perturbs memory formation (Barco and Marie, 2011).

We recently reported that CFC is associated with an increase in the density of dendritic spines in CA1 pyramidal neurons of the hippocampus of WT mice while leading to an elimination of these spines in mCREB mice (Middei et al., 2012). To further investigate the molecular processes underlying this opposite morphological effect, we here measured the learning-driven AMPAR and NMDAR alterations within the PSD. We analyzed how CFC altered the PSD AMPAR and NMDA subunit levels and PSD-95 distribution when evaluated 24 h after the CFC test. This time point after CFC was chosen to correlate this new data with the significant spine loss reported at this same time point in our previous publication (Middei et al., 2012). As shown in Figure 6, CFC did not modify GluA1 levels in total extract in either genotype (Fig. 6A; genotype effect: $F_{1,8} = 4.21$, $P > 0.1$). Blocking CREB function, however, significantly perturbed the learning-induced alterations in GluA1 within the PSD (Figs. 6B–D). CFC induced a significant increase in GluA1 in WT mice within the PSD (Fig. 6B; genotype × training effect, $F_{1,15} = 4.57$, $P < 0.05$, post hoc WT naïve vs. WT CFC $P < 0.01$). This increase in GluA1 within the PSD was a consequence of learning as it was not observed in pseudo-trained WT mice (data not shown). Interestingly, this learning-induced alteration was totally absent in mCREB mice (Fig. 6B, post hoc mCREB naïve vs. mCREB CFC $P > 0.05$; WT CFC vs. mCREB CFC $P < 0.0001$). Also, levels of the GluA1-Ser845 phosphorylated form was increased in the PSD of WT neurons after CFC (Fig. 6C; significant genotype × training condition interaction: $F_{1,17} = 18.65$, $P < 0.001$; WT naïve vs. WT CFC $P < 0.001$). Again, this increase in GluA1-ser845 levels was a consequence of learning as it was not observed in pseudo-trained WT mice (data not shown). This learning-induced alteration was also totally absent in mCREB mice (Fig. 6C; mCREB naïve vs. mCREB CFC, $P > 0.05$; WT CFC vs. mCREB CFC, $P < 0.0001$). CFC induced an increase in the levels of the GluA1-Ser831 phosphorylated form within the PSD in both genotypes (significant effect of training condition: Fig. 6D, $F_{1,15} = 27.79$, $P < 0.001$) as confirmed by post hoc multiple comparisons (WT naïve vs. WT CFC, $P < 0.01$; mCREB naïve vs. mCREB CFC, $P < 0.05$), but this increase was less significant in mCREB mice (WT CFC vs. mCREB CFC, $P < 0.01$). The ratio of the GluA1-Ser845 phosphorylated form versus total GluA1 within the PSD after CFC was, however, not significantly perturbed by loss of CREB function (Fig. 6E, genotype × training effect, $F_{1,15} = 4.29$, $P > 0.05$), nor was the ratio of the GluA1-Ser831 phosphorylated form versus total GluA1 (Fig. 6F, genotype × training effect, $F_{1,15} = 0.38$, $P > 0.05$). Together these data demonstrate that CREB is necessary for the learning-dependent alterations in the levels of GluA1 and GluA1-Ser845, and to a lesser extent of GluA1-Ser831, within the PSD.

We also investigated if loss of CREB function could perturb the learning-induced alterations of other synaptic proteins within the PSD. Analysis of total homogenates revealed that CFC led to a slight but significant reduction in GluA2/3 expression in WT mice but not in mCREB mice (Fig. 7A; significant genotype × training condition interaction: $F_{1,8} = 8.6$, $P < 0.05$; WT naïve vs. WT CFC, $P < 0.05$). The total homogenate levels of all other proteins analyzed (GluN1, GluN2A, and PSD95) were not altered by CFC in either genotype (Figs. 7C,E,G). CFC led to a significant increase in the level of all these proteins within the PSD in both WT and mCREB mice (Figs. 7BD,F,H; training condition effects for GluA2/3: $F_{1,19} = 660.07$, $P < 0.0001$; for GluN1: $F_{1,15} = 66.11$, $P < 0.0001$; for GluN2A: $F_{1,11} = 33.88$, $P < 0.001$; for PSD95: $F_{1,11} = 33.93$, $P < 0.001$). Bonferroni multiple comparisons revealed that these effects were evident in both genotypes (GluR2/3: WT naïve vs. WT CFC, $P < 0.0001$; mCREB naïve vs. mCREB CFC, $P < 0.0001$; GluN1: WT naïve vs. WT CFC $P < 0.0001$; mCREB naïve vs. mCREB CFC, $P < 0.01$; GluN2A: WT naïve vs. WT CFC, $P < 0.01$; mCREB naïve vs. mCREB CFC, $P < 0.05$; PSD95: WT naïve vs. WT CFC, $P < 0.01$; mCREB naïve vs. mCREB CFC, $F_{1,6} = 6.87$, $P < 0.05$). It is worth noting however that this increase was consistently less statistically significant in mCREB mice than in WT mice for all the proteins analyzed. These data demonstrate that loss of CREB function specifically affects GluA1-related learning-dependent alterations within the PSD, and might also partially influence the learning-dependent modifications of other synaptic proteins within the PSD.

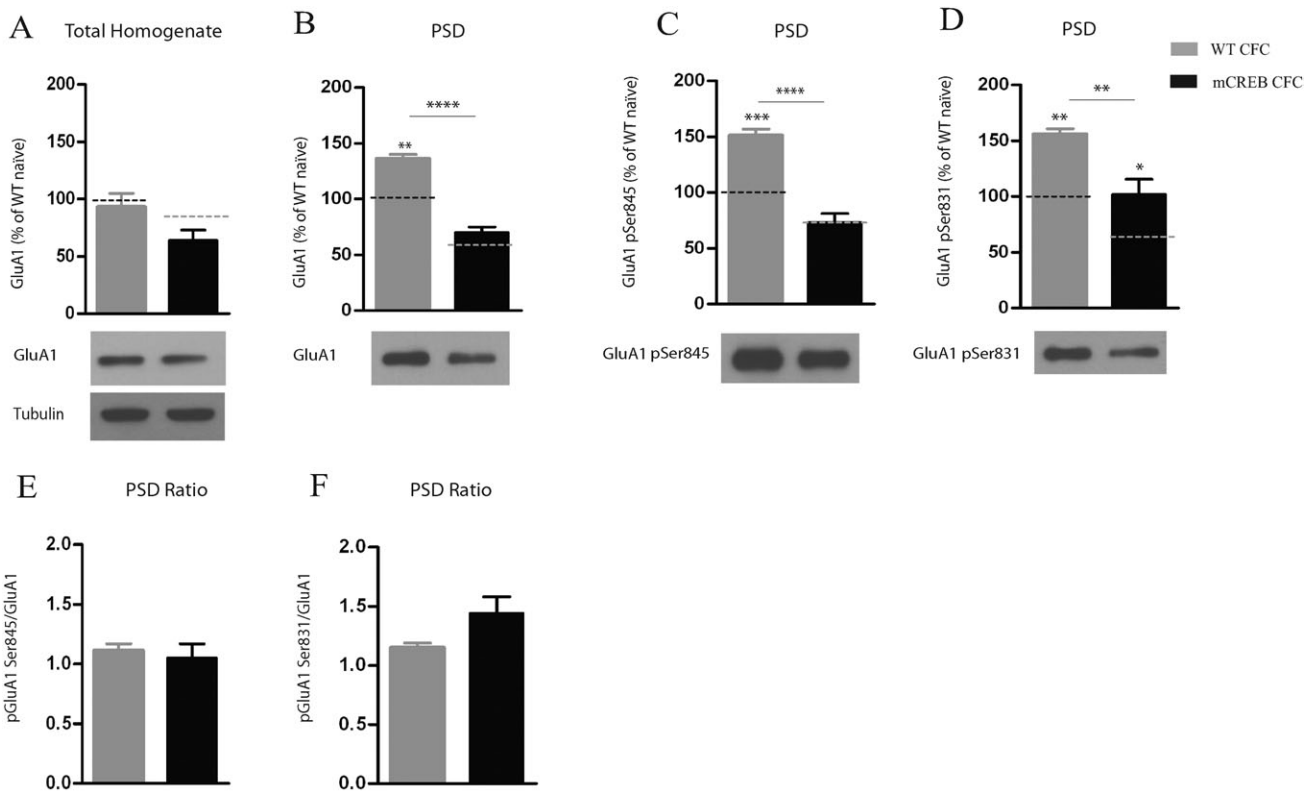

FIGURE 6. CREB is necessary for learning-induced alterations of GluA1 within the PSD. Quantitative analysis of GluA1 and its phosphorylated forms (S845 and S831) in the hippocampus of mCREB and WT mice 24 h after CFC. (A-D) Densitometric quantification of changes in gray values expressed as mean (% of average WT naïve) ± s.d. and representative immunoblots used for quantification. Dotted lines correspond to naïve averages of WT and mCREB from Figure 2. (A) GluA1 levels in total hippocampal extracts (tubulin was used for normalization for total homogenates); (B) GluA1 levels in the PSD; (C) Levels of S845 phosphorylated GluA1 in the PSD; (D) Levels of S831 phosphorylated GluA1 in the PSD; (n = 3 mice in each group for total homogenates, n = 4/5 mice in each group for PSDs). (E) Ratio of S845 phosphorylated GluA1 in PSD (data from C) to GluA1 in the PSD (data from B). (F) Ratio of S831 phosphorylated GluA1 in PSD (data from D) to GluA1 in the PSD (data from B). *$P < 0.05$, **$P < 0.01$, ***$P < 0.001$, ****$P < 0.0001$.

Doxy administration rescues phenotypic alterations in mCREB mice.

We previously reported that shutting down mCREB expression in adult mCREB mice with 10 days of doxycycline administration rescues from CFC memory impairment and restores CFC-induced dendritic spines dynamics (Middei et al., 2012). Here, we investigated whether briefly inhibiting mCREB expression with doxy treatment would prevent alterations in GluA1 levels and synaptic plasticity. WT mice received an identical doxy diet for these experiments. First, we confirmed that shutting down mCREB expression prevents memory deficits in mCREB mice (Middei et al., 2012). We tested mCREB and WT mice in CFC after 10 days of doxy treatment. The two groups of mice exhibited similar freezing behaviors during both the training ($F_{1,4} = 3.95$, $P > 0.05$) and test ($F_{1,4} = 0.02$, $P > 0.05$) (Supporting Information Fig. S2A). We then analyzed the levels of the AMPAR GluA1 subunit within the PSD in naïve and CFC WT and mCREB mice after doxy treatment. We observed that GluA1 levels were unaffected in mCREB mice in naïve conditions (effect of genotype: $F_{1,10} = 3.82$, $P > 0.05$), and that CFC induced a significant increase in GluA1 levels in both mCREB and WT mice (effect of training condition: $F_{1,10} = 421.17$, $P > 0.05$) (Supporting Information Fig. S2B), demonstrating that the GluA1 phenotypic alterations observed in untreated mCREB mice are entirely dependent on mCREB expression. Also, the observed LTD change induced by chronic inhibition of CREB was absent in mCREB mice submitted to the doxy diet (Supporting Information Figs. S2C–D). Altogether, these data demonstrate that the observed synaptic perturbations induced by chronic deprivation of CREB function are not permanent and can be restored within days by shutting down mCREB expression.

DISCUSSION

Synaptic strengthening in the hippocampus constitutes a major molecular basis for memory storage (Kasai et al., 2010). This process involves phosphorylation and trafficking of AMPARs to activated synapses (Lu and Roche, 2012), and

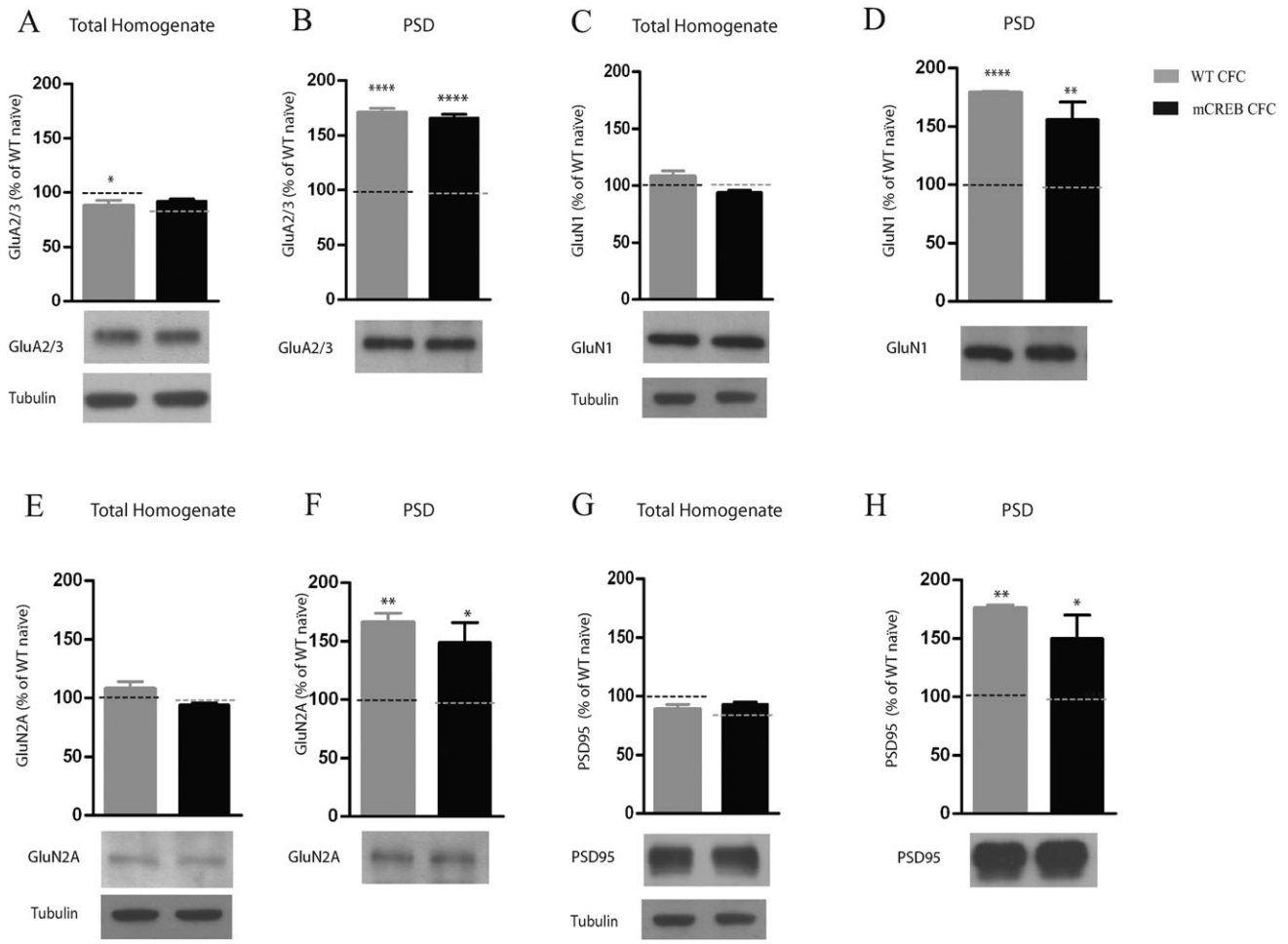

FIGURE 7. Blocking CREB function does not alter the learning-induced incorporation of other synaptic proteins within the PSD. Quantitative analysis of GluA2/3, GluN1, GluN2A, and PSD95 in the hippocampus of mCREB and WT mice 24 h after CFC. (A–H) Densitometric quantification of changes in gray values expressed as mean (% of average WT naïve) ± s.d. and representative immunoblots used for quantification. Dotted lines correspond to naïve averages of WT and mCREB from Figure 3. (A) GluA2/3 levels in total hippocampal extracts (tubulin was used for normalization for total homogenates); (B) GluA2/3 levels in the PSD; (C) GluN1 levels in total hippocampal extracts; (D) GluN1 levels in the PSD; (E) GluN2A levels in total hippocampal extracts; (F) GluN2A levels in the PSD; (G) PSD95 levels in total hippocampal extracts; (H) PSD95 levels in the PSD; ($n = 3$ mice in each group for total homogenates and PSD analysis of PSD95, $n = 4/6$ mice in each group for all other PSD analyses). $^{*}P < 0.05$, $^{**}P < 0.01$, $^{***}P < 0.001$, $^{****}P < 0.0001$.

activation of intracellular signalling pathways resulting in actin cytoskeleton rearrangements that stabilize dendritic spines which are proposed to "lock in" the synaptic changes (Cingolani and Goda, 2008). The role of the transcription factor CREB in these events had not previously been investigated. In a recent report, we showed that CREB is necessary for the learning-induced spine and actin rearrangements driving CFC (Middei et al., 2012). Here, we confirmed that inhibiting CREB function in adult mice perturbs CFC and lowers LTP in CA1 hippocampal neurons, as previously shown by us and others (Kida et al., 2002; Pittenger et al., 2002; Huang et al., 2004; Jancic et al., 2009; Mamiya et al., 2009; Middei et al., 2012). More importantly, we now demonstrated that CREB is required to maintain the AMPAR subunit GluA1 within the PSD under basal conditions. We corroborated these biochemical data with electrophysiological data demonstrating that CREB is necessary to maintain AMPAR synaptic transmission in CA1 pyramidal neurons under basal conditions. We also showed that CREB is necessary for the learning-induced insertion of GluA1 within the PSD. These CREB-dependent regulations were specific for GluA1 since the PSD levels of the AMPARs subunits GluA2/3 as well as the NMDARs subunits GluN1 and GluN2A and of PSD-95 in basal and learning-induced conditions were normal. These data argue for an important role of CREB in regulating AMPAR trafficking at the synapse, as the majority (80%) of AMPAR-containing synapses of CA1 pyramidal neurons expresses GluA1 (Lu et al., 2009). At present, we however cannot confirm if the role of CREB in AMPAR trafficking is direct or ancillary to other processes affected by CREB. Our data suggest that CREB does not directly control GluA1 gene expression since GluA1 levels in total hippocampal homogenates were not different in mCREB

and WT mice. It is more likely that CREB regulates the expression of other proteins implicated in AMPAR trafficking, such as for example the brain derived neurotrophic factor BDNF, a well-known CREB target (Shieh et al., 1998), or the immediate early gene Arc (Kawashima et al., 2009). Both of these proteins have been shown to regulate AMPAR trafficking (Caldeira et al., 2007; Bramham et al., 2008).

Phosphorylation events of this subunit at serine 845 and serine 831 are known to be involved in plasticity processes such as LTP and LTD (Lee et al., 2000; Lu and Roche, 2012). We showed that inhibiting CREB strongly affected the GluA1 Serine 845 phosphorylated form. Indeed, we found that in basal conditions, loss of CREB function enhanced the proportion of this phosphorylated form within the PSD. We also found that loss of CREB function prevented any further increase in this phosphorylated form within the PSD that normally occurs with learning. Dephosphorylation of serine 845 is known to be important for LTD. Consistently, we observed an enhanced LTD when induced at SC-CA1 synapses of mCREB mice. Less influence of CREB was evident for the serine 831 phosphorylated form, the importance of which in plasticity processes is still unclear (Lu and Roche, 2012). The subtle alterations in GluA1-serine 831 PSD levels together with the strong alterations in GluA1-serine 845 PSD levels observed in the mCREB mice could contribute to the deficits in LTP we observed as there is evidence that disruption of both phosphorylation sites is necessary to perturb hippocampal LTP (Lee et al., 2003). The principal kinase involved in serine 845 phosphorylation is protein kinase A (PKA), while protein kinase C and CamKII regulate phosphorylation at serine 831 (Lu and Roche, 2012). It is interesting to note that of these kinases, only PKA phosphorylates and activates CREB. One could therefore envisage that disrupting CREB function could alter a yet unknown feedback mechanism whereby CREB activity is involved in PKA-dependent regulation of GluA1 phosphorylation.

We and others previously demonstrated that enhancing CREB function increases NMDAR transmission and the surface levels of NMDAR subunits (Marie et al., 2005; Huang et al., 2008). Huang et al. (2008) further reported that brief in vivo expression of mCREB (CREBS133A) in medium spiny neurons of the nucleus accumbens did not alter AMPAR function nor NMDAR function (Huang et al., 2008). Our chronic inhibition of CREB, by expression of mCREB in hippocampal neurons, specifically perturbed AMPAR levels within the PSD without altering the levels of the principal subunits of the NMDAR (GluN1 and GluN2A). It is therefore likely that, unlike the effect of CREB on intrinsic excitability which consists of a clear bidirectional regulation in all neurons studied (Pittenger et al., 2002; Dong et al., 2006; Han et al., 2006; Lopez et al., 2007; Jancic et al., 2009; Viosca et al., 2009; Zhou et al., 2009), CREB-dependent regulation of synaptic receptors will be more complex. It could depend on the length of activation or inhibition (chronic or brief) of CREB and/or the type of neuron analyzed.

In summary, we provide the first evidence that CREB has a pivotal role in controlling the GluA1 trafficking in the PSD of hippocampal neurons under basal conditions and during synaptic strengthening sub-serving the persistence of long term memory.

Acknowledgments

The authors thank Ronald Duman (Yale University) for donating the mCREB transgenic mice.

REFERENCES

Barco A, Marie H. 2011. Genetic approaches to investigate the role of CREB in neuronal plasticity and memory. Mol Neurobiol 44:330–349.

Barco A, Alarcon JM, Kandel ER. 2002. Expression of constitutively active CREB protein facilitates the late phase of long-term potentiation by enhancing synaptic capture. Cell 108:689–703.

Bramham CR, Worley PF, Moore MJ, Guzowski JF. 2008. The immediate early gene arc/arg3.1: Regulation, mechanisms, and function. J Neurosci 28:11760–11767.

Caldeira MV, Melo CV, Pereira DB, Carvalho R, Correia SS, Backos DS, Carvalho AL, Esteban JA, Duarte CB. 2007. Brain-derived neurotrophic factor regulates the expression and synaptic delivery of alpha-amino-3-hydroxy-5-methyl-4-isoxazole propionic acid receptor subunits in hippocampal neurons. J Biol Chem 282:12619–12628.

Carlezon WA, Duman RS, Nestler EJ. 2005. The many faces of CREB. Trends Neurosci 28:436–445.

Cingolani LA, Goda Y. 2008. Actin in action: The interplay between the actin cytoskeleton and synaptic efficacy. Nat Rev Neurosci 9:344–356.

D'Amelio M, Cavallucci V, Middei S, Marchetti C, Pacioni S, Ferri A, Diamantini A, De ZD, Carrara P, Battistini L, Moreno S, Bacci A, Ammassari-Teule M, Marie H, Cecconi F. 2011. Caspase-3 triggers early synaptic dysfunction in a mouse model of Alzheimer's disease. Nat Neurosci 14:69–76.

Dong Y, Green T, Saal D, Marie H, Neve R, Nestler EJ, Malenka RC. 2006. CREB modulates excitability of nucleus accumbens neurons. Nat Neurosci 9:475–477.

Han MH, Bolanos CA, Green TA, Olson VG, Neve RL, Liu RJ, Aghajanian GK, Nestler EJ. 2006. Role of cAMP response element-binding protein in the rat locus ceruleus: regulation of neuronal activity and opiate withdrawal behaviors. J Neurosci 26:4624–4629.

Huang YH, Lin Y, Brown TE, Han MH, Saal DB, Neve RL, Zukin RS, Sorg BA, Nestler EJ, Malenka RC, Dong Y. 2008. CREB modulates the functional output of nucleus accumbens neurons: a critical role of N-methyl-D-aspartate glutamate receptor (NMDAR) receptors. J Biol Chem 283:2751–2760.

Huang YY, Pittenger C, Kandel ER. 2004. A form of long-lasting, learning-related synaptic plasticity in the hippocampus induced by heterosynaptic low-frequency pairing. Proc Natl Acad Sci USA 101:859–864.

Jancic D, Lopez de AM, Valor LM, Olivares R, Barco A. 2009. Inhibition of cAMP response element-binding protein reduces neuronal excitability and plasticity, and triggers neurodegeneration. Cereb. Cortex 19:2535–2547.

Kasai H, Fukuda M, Watanabe S, Hayashi-Takagi A, Noguchi J. 2010. Structural dynamics of dendritic spines in memory and cognition. Trends Neurosci 33:121–129.

Kawashima T, Okuno H, Nonaka M, Adachi-Morishima A, Kyo N, Okamura M, Takemoto-Kimura S, Worley PF, Bito H. 2009. Synaptic activity-responsive element in the Arc/Arg3.1 promoter

essential for synapse-to-nucleus signaling in activated neurons. Proc Natl Acad Sci USA 106,316–321.

Kida S, Josselyn SA, Pena de OS, Kogan JH, Chevere I, Masushige S, Silva AJ. 2002. CREB required for the stability of new and reactivated fear memories. Nat Neurosci 5:348–355.

Lee HK, Barbarosie M, Kameyama K, Bear MF, Huganir RL. 2000. Regulation of distinct AMPA receptor phosphorylation sites during bidirectional synaptic plasticity. Nature 405:955–959.

Lee HK, Takamiya K, Han JS, Man H, Kim CH, Rumbaugh G, Yu S, Ding L, He C, Petralia RS, Wenthold RJ, Gallagher M, Huganir RL. 2003. Phosphorylation of the AMPA receptor GluR1 subunit is required for synaptic plasticity and retention of spatial memory. Cell 112:631–643.

Lopez de Armentia M, Jancic D, Olivares R, Alarcon JM, Kandel ER, Barco A. 2007. cAMP response element-binding protein-mediated gene expression increases the intrinsic excitability of CA1 pyramidal neurons. J Neurosci 27:13909–13918.

Lu W, Roche KW. 2012. Posttranslational regulation of AMPA receptor trafficking and function. Curr Opin Neurobiol 22:470–479.

Lu W, Shi Y, Jackson AC, Bjorgan K, During MJ, Sprengel R, Seeburg PH, Nicoll RA. 2009. Subunit composition of synaptic AMPA receptors revealed by a single-cell genetic approach. Neuron 62:254–268.

Malenka RC, Bear MF. 2004. LTP and LTD: an embarrassment of riches. Neuron 44,5–21.

Mamiya N, Fukushima H, Suzuki A, Matsuyama Z, Homma S, Frankland PW, Kida S. 2009. Brain region-specific gene expression activation required for reconsolidation and extinction of contextual fear memory. J Neurosci 29:402–413.

Marchetti C, Tafi E, Marie H. 2011. Viral-mediated expression of a constitutively active form of cAMP response element binding protein in the dentate gyrus increases long term synaptic plasticity. Neuroscience 190:21–26.

Marchetti C, Tafi E, Middei S, Rubinacci MA, Restivo L, Ammassari-Teule M, Marie H. 2010. Synaptic adaptations of CA1 pyramidal neurons induced by a highly effective combinational antidepressant therapy. Biol Psychiatry 67:146–154.

Marie H, Morishita W, Yu X, Calakos N, Malenka RC. 2005. Generation of silent synapses by acute in vivo expression of CaMKIV and CREB. Neuron 45:741–752.

Matsuo N, Reijmers L, Mayford M. 2008. Spine-type-specific recruitment of newly synthesized AMPA receptors with learning. Science 319:1104–1107.

Mayford M, Bach ME, Huang YY, Wang L, Hawkins RD, Kandel ER. 1996. Control of memory formation through regulated expression of a CaMKII transgene. Science 274:1678–1683.

Middei S, Spalloni A, Longone P, Pittenger C, O'Mara SM, Marie H, Ammassari-Teule M. 2012. CREB selectively controls learning-induced structural remodeling of neurons. Learn Mem 19,330–336.

Newton SS, Thome J, Wallace TL, Shirayama Y, Schlesinger L, Sakai N, Chen J, Neve R, Nestler EJ, Duman RS. 2002. Inhibition of cAMP response element-binding protein or dynorphin in the nucleus accumbens produces an antidepressant-like effect. J Neurosci 22:10883–10890.

Pittenger C, Huang YY, Paletzki RF, Bourtchouladze R, Scanlin H, Vronskaya S, Kandel ER. 2002. Reversible inhibition of CREB/ATF transcription factors in region CA1 of the dorsal hippocampus disrupts hippocampus-dependent spatial memory. Neuron 34:447–462.

Restivo L, Tafi E, Ammassari-Teule M, Marie H. 2009. Viral-mediated expression of a constitutively active form of CREB in hippocampal neurons increases memory. Hippocampus 19:228–234.

Rumpel S, LeDoux J, Zador A, Malinow R. 2005. Postsynaptic receptor trafficking underlying a form of associative learning. Science 308:83–88.

Sekeres MJ, Neve RL, Frankland PW, Josselyn SA. 2010. Dorsal hippocampal CREB is both necessary and sufficient for spatial memory. Learn Mem 17:280–283.

Shieh PB, Hu SC, Bobb K, Timmusk T, Ghosh A. 1998. Identification of a signaling pathway involved in calcium regulation of BDNF expression. Neuron 20:727–740.

Viosca J, Lopez de AM, Jancic D, Barco A. 2009. Enhanced CREB-dependent gene expression increases the excitability of neurons in the basal amygdala and primes the consolidation of contextual and cued fear memory. Learn Mem 16:193–197.

Zhou Y, Won J, Karlsson MG, Zhou M, Rogerson T, Balaji J, Neve R, Poirazi P, Silva AJ. 2009. CREB regulates excitability and the allocation of memory to subsets of neurons in the amygdala. Nat Neurosci 12:1438–1443.